HHS Public Access

Author manuscript

Org Lett. Author manuscript; available in PMC 2020 April 05.

Published in final edited form as:

Org Lett. 2019 April 05; 21(7): 2412–2415. doi:10.1021/acs.orglett.9b00707.

Troponoid Atropisomerism: Studies on the Configurational Stability of Tropone-Amide Chiral Axes

Danielle R. Hirsch[a,b], **Anthony J. Metrano**[c], **Elizabeth A. Stone**[c], **Golo Storch**[c], **Scott J. Miller**[*,c], and **Ryan P. Murelli**[*,a,b]

[a]Department of Chemistry, Brooklyn College, The City University of New York, Brooklyn, New York 11210, United States

[b]PhD Program in Chemistry, The Graduate Center of the City University of New York, New York, New York 10016 United States

[c]Department of Chemistry, Yale University, New Haven, Connecticut 06520-8107, United States

Abstract

Configurationally stable, atropisomeric motifs are an important structural element in a number of molecules, including chiral ligands, catalysts, and molecular devices. Thus, understanding features that stabilize chiral axes is of fundamental interest throughout the chemical sciences. The following details the high rotational barriers about the Ar–C(O) bond of tropone amides, which significantly exceed those of analogous benzamides. These studies are supported by both experimental and computational rotational barrier measurements. We also report the resolution of an axially chiral α-hydroxytropolone amide into its individual atropisomers, and demonstrate its configurational stability at physiological pH and temperatures over 24 hours.

Graphical Absract:

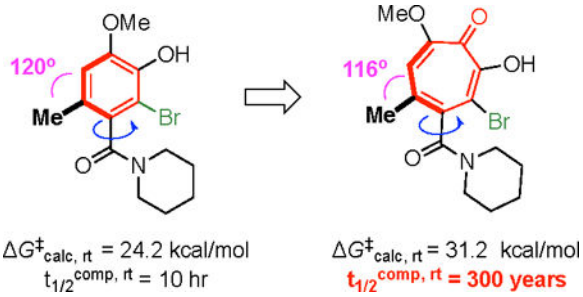

Atropisomerism, a form of chirality arising from restricted rotation about an asymmetric axis, plays an important role in a number of functional molecules[1] including chiral biaryl ligands and catalysts (e.g., **1**,[2] Figure 1A),[3] as well as unidirectional molecular devices and switches.[4] Single atropisomer therapeutics also exist, although they often have their roots in

[*]**Corresponding Authors:** rpmurelli@brooklyn.cuny.edu, scott.miller@yale.edu.

Supporting Information

Supporting information including detailed experimental procedures and ^{1}H and ^{13}C NMR spectra. These materials are available free of charge via the Internet at http://pubs.acs.org.

natural products (e.g., **2**,[5] Figure 1A).[6] However, given the critical importance of chirality in drug development, they are also becoming increasingly prevalent in *de novo* drug design (e.g., **3**,[7] Figure 1A).[8] Compared to 5- and 6-membered aromatic rings commonly found in drugs, troponoids should have an increased likelihood of being atropisomeric due to their decreased external bond angles (Figure 1B). However, other features such as tropylium characteristics,[9] ring puckering,[10] and decreased aromaticity[11] could influence the rotational barriers, as well. Only a few troponoids are known to exhibit atropisomerism, including colchicine (**2**, Figure 1A, $\Delta G^{\ddagger}_{298\ K}$ = 22 kcal/mol)[5] and bistropone homodimer **4** (Figure 1C, $\Delta G^{\ddagger}_{298\ K}$ = 20.7 kcal/mol),[12] both of which have relatively low rotational barriers. Given the growing interest in troponoid drug development,[13] as well as the importance of atropisomerism throughout the chemical sciences, understanding how this motif influences atropisomerism compared to benzenoids would be helpful in designing new, functional atropisomeric molecules.

Our investigation began with DFT computations on a series of axially chiral tropolones and analogous benzenoids (Table 1).[14] Troponoid substrates consistently exhibited higher rotational barriers than those of the corresponding benzenoids, with rotational energy barrier increases of up to 4.3 kcal/mol (**Entry 4**), and increases in half-lives to enantiomerization at room temperature of up to four orders of magnitude.

To confirm these energy barriers experimentally, we turned to α-hydroxytropolone **7** and benzamide **8** (Figure 2A, B), which were readily accessible from the corresponding carboxylic acids.[15,16] ^{1}H NMR spectra of these molecules have diagnostic diastereotopic signals and observable *E* and *Z* amide isomers useful for probing the configurational stability of the Ar–C(O) and N–C(O) axes, respectively, through variable temperature NMR experiments (Figure 2A, B). Prior studies on hindered benzamides have established that, in addition to isolated Ar–C(O) and N–C(O) rotations, isomerization can also proceed through an often energetically intermediate, concerted Ar–C(O)/N–C(O) process (Figure 2C).[17] Consistent with this precedent, computational modeling on both **7** and **8** revealed that Ar–C(O) rotational barriers were lower in energy than N–C(O) rotation, and the concerted Ar–C(O)/N–C(O) rotation was the lowest energy pathway for effective N–C(O) amide isomerization (Figure 2C). These results were also validated by variable temperature NMR experiments. Heating a solution of **7** in DMSO-*d*6 led to coalescence of only the diastereotopic signals, which allowed us to measure the individual rotational energy barriers of the Ar–C(O) bonds of both *E* and *Z* isomers ($\Delta G^{\ddagger}_{E}$ = 16.7 kcal/mol, $\Delta G^{\ddagger}_{Z}$ =16.5 kcal/mol). Conversely, cooling a sample of **8** revealed proton diastereotopicity, and allowed an experimental Ar–C(O) rotational barrier measurement ($\Delta G^{\ddagger}_{E}$ = 12.2 kcal/mol, $\Delta G^{\ddagger}_{Z}$ = 12.1 kcal/mol, Figure 2B). Finally, while no coalescence of the amide rotamers of **7** was observed at higher temperatures, heating a solution of **8** in DMSO-d_6 to 90 °C led to complete coalescence of its amide rotamers (Figure 2B). The increased stability of the N–C(O) axis of **7** relative to **8** demonstrates the ancillary rigidity provided by the tropone.

In order to observe these rotational barrier differences in more configurationally stable systems, we modeled brominated variants of the compounds shown in Table 1 (Figure 3A).[7,14,18] Rotational barriers increased by upwards of 11 kcal/mol for the benzenoids and by 14 kcal/mol for the troponoids. A corollary of this effect is observed in the half-life to

enantiomerization of **10c**, which was computed to take place over centuries at room temperature ($t_{½,\ 298\ K}$ = ~300 years), relative to hours for benzenoid **9c** ($t_{½,\ 298\ K}$ = ~10 hours). Based on the classification system put forward by LaPlante and co-workers, these two molecules are considered to be class 3 ($\Delta G^{‡}$ > 28 kcal/mol) and class 2 ($\Delta G^{‡}$ ≈ 20–28 kcal/mol) atropisomers, respectively (Figure 3B).[19] Class 2 molecules fall into a category where the molecules are atropisomeric, but the rotational barriers might not be high enough to develop them as single atropisomers. Class 3 molecules are those with rotational barriers sufficiently high to confidently develop as single-atropisomer drugs.

To obtain the quantities of enantioenriched **10c** necessary to confirm these high energy barriers experimentally, we turned our attention to a peptide-catalyzed dynamic kinetic atroposelective halogenation[14,18,20] that had been established on structurally analogous benzamides (*i.e.* **11** vs. **6c**, Figure 4A/B).[20a] Employing slightly modified conditions to those used previously on **11**, we were able to obtain **10c** in 75:25 er.[21] We next monitored enantioerosion of a solution of enantioenriched **10c** (93:7 er) in triglyme over 60 minutes at 145 °C, and obtained an experimental energy barrier of 30.1 kcal/mol.[16] A discrepancy between this value and that computed using DFT at the same temperature ($\Delta G^{‡}_{418\ K}$ = 32.7 kcal/mol) may be due to the triglyme solvent.

Methoxytropolones, such as **10c**, are known precursors to α-hydroxytropolones,[22] which are promising dinuclear metalloenzyme-inhibiting fragments we have been leveraging in drug-development pursuits for a number of different diseases.[23] The high energy barriers we identified for **10c** suggested that structurally analogous α-hydroxytropolones could be studied as single atropisomers. α-Hydroxytropolone **15** was thus synthesized through demethylation of **10c** and resolved into individual enantiomers with a preparatory scale chiral stationary phase column.[16] To test stability under physiological conditions, an enantiomerically enriched sample consisting of 93% **(−)-15** and 7% **(+)-15** was dissolved in phosphate buffer (pH = 7.4) and heated to 37 °C for 24 hours; no change was observed in the enantiomeric ratio over this time period (Figure 4**E**). This result is important for tropolone development as single atropisomers, since ionization states can change rotational barriers[24] and tropolones are likely to exist in an anionic state at physiological pH.[25]

In conclusion, computational and experimental rotational barrier measurements demonstrate that tropone-amide chiral axes are substantially higher than those of analogous benzamides. We also synthesized and resolved a configurationally stable, axially chiral α-hydroxytropolone amide, and we found the enantiomers to be stable at physiological temperature and pH for over 24 hrs. Given the importance of configurationally stable atropisomeric molecules throughout the chemical sciences, these studies suggest that tropones could find a valuable role in atropisomeric molecule design.

Supplementary Material

Refer to Web version on PubMed Central for supplementary material.

ACKNOWLEDGMENT

This work is supported by the National Institute of General Medicinal Sciences of the United States National Institutes of Health in the form of Grants to RPM (SC1GM111158) and SJM (R37GM068649). DRH was supported by the CUNY Mina Rees Dissertation Fellowship. AJM was supported by the NSF Graduate Research Fellowship Program. EAS acknowledges the NIH Molecular Biophysical Predoctoral Training Grant (T32 GM008283) and the NSF Graduate Research Fellowship Program for research support. GS is grateful to the Deutsche Forschungsgemeinschaft (DFG) for a postdoctoral fellowship (STO 1175/1–1). We also want to thank Dr. Sean Colvin (Yale University) and John Stasiak (Brooklyn College) for technical assistance.

REFERENCES

(1). (a)For lead reviews, see: Kumarasamy E; Raghunathan R; Sibi MP; Sivaguru, J. Chem. Rev 2015, 115, 11239–300.(b) Gluntz PW Biorg. Med. Chem. Lett 2018, 28, 53–60.

(2). Meca L; Řeha D; Havlas ZJ Org. Chem 2003, 68, 5677– 80.

(3). (a)Tang W; Zhang X Chem. Rev 2003, 103, 3029–3069. [PubMed: 12914491] (b)Cardo-so FSP; Abboud KA; Aponick AJ Am. Chem. Soc 2013, 135, 14548–51.(c)Fernández E; Guiry PJ; Connole KP; Brown JM J. Org. Chem 2014, 79, 5391–400. [PubMed: 24806741]

(4). (a)For lead examples, see: Kelly TR; De Silva H; Silva RA Nature 1999, 401, 150–152. [PubMed: 10490021] (b)Collins BSK; Kistemaker JCM; Otten E; Feringa BL Nat. Chem 2016, 8, 860–866. (c)Feringa BL; Koumura N; Zijlstra RWJ; Van Delden RA; Harada N Nature, 1999, 401, 152–155. [PubMed: 10490022]

(5). (a)Hartung E Ann Rhem. Dis 1954, 13, 190–200.(b)Brossi A; Yeh HJ; Chrzanowska M; Wolff J; Hamel E; Lin CM; Quin F; Suffness M; Silverton J Med. Res. Rev 1988, 8, 77–94. [PubMed: 3278182]

(6). Zask A; Murphy J; Ellestad GA Chirality, 2013, 25, 265–274. [PubMed: 23620262]

(7). Smith DE; Marquez I; Lokensgard ME; Rheingold AL; Hecht DA; Gustafson JL Angew. Chem. Int. Ed 2015, 54, 11754–11759.

(8). (a)For select recent examples, see: Chandrasekhar J; Dick R; Van Veldhuizen J; Koditek D; Lepist E-Ir; McGrath ME; Patel L; Phillips G; Sedillo K; Somoza JR; Therrien J; Till NA; Treiberg J; Villasenor AG; Zherebina Y; Perreault S J. Med. Chem 2018, 61, 6858–6868.. [PubMed: 30015489] (b)Beutner G; Carrasquillo R; Geng P; Hsaio Y; Huang EC; Janey J; Katipally K; Kolotuchin S; La Porte T; Lee A; Lobben P; Lora-Gonzalez F; Mack B; Mudryk B; Qiu Y; Qian X; Ramirez A; Razler TM; Rosner T; Shi Z; Simmons E; Stevens J; Wang J; Wei C; Wisniewski SR; Zhu Y Org. Lett 2018, 20, 3736– 3740 [PubMed: 29909639] (c)Fordyce EAF; Fraser Hunt S; Crepin D; Onions ST; Parra GF; Sleigh CJ; King-Underwood J; Finch H; Murray J Med. Chem. Commun 2018, 9, 583–589.For recent review, see: (d) Toenjes ST; Gustafson JL Future Med. Chem 2018, 10, 409–422. [PubMed: 29380622]

(9). Pauson PL Chem. Rev 1955, 55, 9–136.

(10). Morita H; Matsumoto K; Takeya K; Itokawa H Chem. Pharm. Bull 1993, 41, 1478–1480. [PubMed: 8403094]

(11). Williams RV; Edwards WD; Zhang P; Berg DJ; Mitchell RH J. Am. Chem. Soc 2012, 134, 16742–16752. [PubMed: 22998507]

(12). Cavazza M; Cifelli M; Domenici B; Funaioli T; Munnucci B; Veracini CA; Zandomeneghi M Chirality, 2013, 25, 648–655. [PubMed: 23828068]

(13). (a)For some lead examples, see: Sennari G; Saito R; Hirose T; Iwatsuki M; Ishayama A; Hokari R; Otoguro K; Omura S; Sunazuka T Sci. Rep 2017, 7, 7259. [PubMed: 28775291] (b)Donlin MJ; Zunica A; Lipnicky A; Garimallaprabhakaran AK; Berkowitz AJ; Grigoryan A; Meyers MJ; Tavis JE; Murelli RP Antimicrob. Agents Chemother 2017, 61, e02574–16. [PubMed: 28167553] (c)Sato D Tayuka K; Kiminori O Bioorg. Med. Chem 2018, 26, 536–42. [PubMed: 29274704] For a review, see: (d) Meck C; D'Erasmo MP; Hirsch DR; Murelli RP Med. Chem. Comm 2014, 5, 842–852.

(14). Barrett KT; Metrano AJ; Rablen PR; Miller SJ Nature, 2014, 509, 71–75. [PubMed: 24747399]

(15). Berkowitz AJ; Abdelmessih RG; Murelli RP Tetrahedron Lett 2018, 59, 3026–208. [PubMed: 30872871]

(16). See supporting information for details.

(17). (a)Ahmed A; Bragg RA; Clayden J; Lai LW; McCarthy C; Pink JH; Westlund N; Yasin SA Tetrahedron, 1998, 54, 13277–13294.(b)Bragg RA; Clayden J; Morris GA; Pink JH Chem. Eur. J 2002, 8, 1279–89. [PubMed: 11921211] (c)Bragg RA; Clayden J Org. Lett 2000, 2, 3351–4; [PubMed: 11029208] (d)Clayden J; Pink JH Angew. Chem., Int. Ed 1998, 37, 1937–9.

(18). (a)For examples, see: Miyaji R; Asano K; Matsubara S J. Am. Chem. Soc 2015, 137, 6766–9. [PubMed: 26000800] (b)Stodulski M; Kohlkepp SV; Raabe G; Gulder T Eur. J. Org. Chem 2016, 137, 6766–6769.

(19). LaPlante SR; Fader LD; Fandrick DR; Hucke I; Kemper R; Miller SPF; Edwards PJ J. Med. Chem 2011, 54, 7005–7022. [PubMed: 21848318]

(20). (a)Barrett KT; Miller SJ J. Am. Chem. Soc 2013, 135, 2963–2966. [PubMed: 23410090] (b)Diener ME; Metrano AJ; Kusano S; Miller SJ J. Am. Chem. Soc 2015, 137, 12369–12377. [PubMed: 26343278] (c)Gustafson JL; Lim D; Barrett KT; Miller SJ Angew. Chem. Int. Ed 2011, 50, 5125–5129.(d)Gustafson J; Lim D; Miller SJ Science, 2010, 328, 1251–1255. [PubMed: 20522769]

(21). (−)-15 is the major enantiomer following demethylation of enantioenriched **10c** acquired through the peptide-catalyzed atroposelective bromination. Thus, **10c** and **(−)-15** are drawn with their absolute stereochemistry established for that of benzamide **12** obtained using analogous conditions described in reference 20a.

(22). Meck C; Mohd N; Murelli RP Org. Lett 2012, 14, 5988–5991. [PubMed: 23167954]

(23). (a)For recent studies, see: Hirsch DR; Schiavone DV; Berkowitz AJ; Morrison LA; Masaoka T; Wilson JA; Lomonosova E; Zhao H; Patel BS; Dalta SH; Majidi SJ; Pal R;K; Gallicchio E; Tang L; Tavis JE; Le Grice SFJ; Beutler JA; Murelli RP Org. Biomol. Chem 2018, 16, 62–69. (b)Dehghanpir SD; Birkenheuer CH; Yang K; Murelli RP; Morrison LA; Le Grice SFJ; Baines JD Vet. Microbiol 2018 214, 125–131. [PubMed: 29408023] (c)Long KR; Lomonosova E; Li Q; Ponzar NL; Villa JA; Touchette E; Rapp S; Liley RM; Murelli RP; Grigoryan A; Buller RM; Wilson L; Bial J; Sagartz JE; Tavis JE Antiviral Res, 2018, 149, 41–47. [PubMed: 29129708]

(24). Welch CJ; Biba M; Pye P; Angelaud R; Egertson MJ Chromatogr. B 2008, 875, 111–121.

(25). Yui N Sci. Rep. Tohoku Univ. First Ser 1956, 40, 114–120.

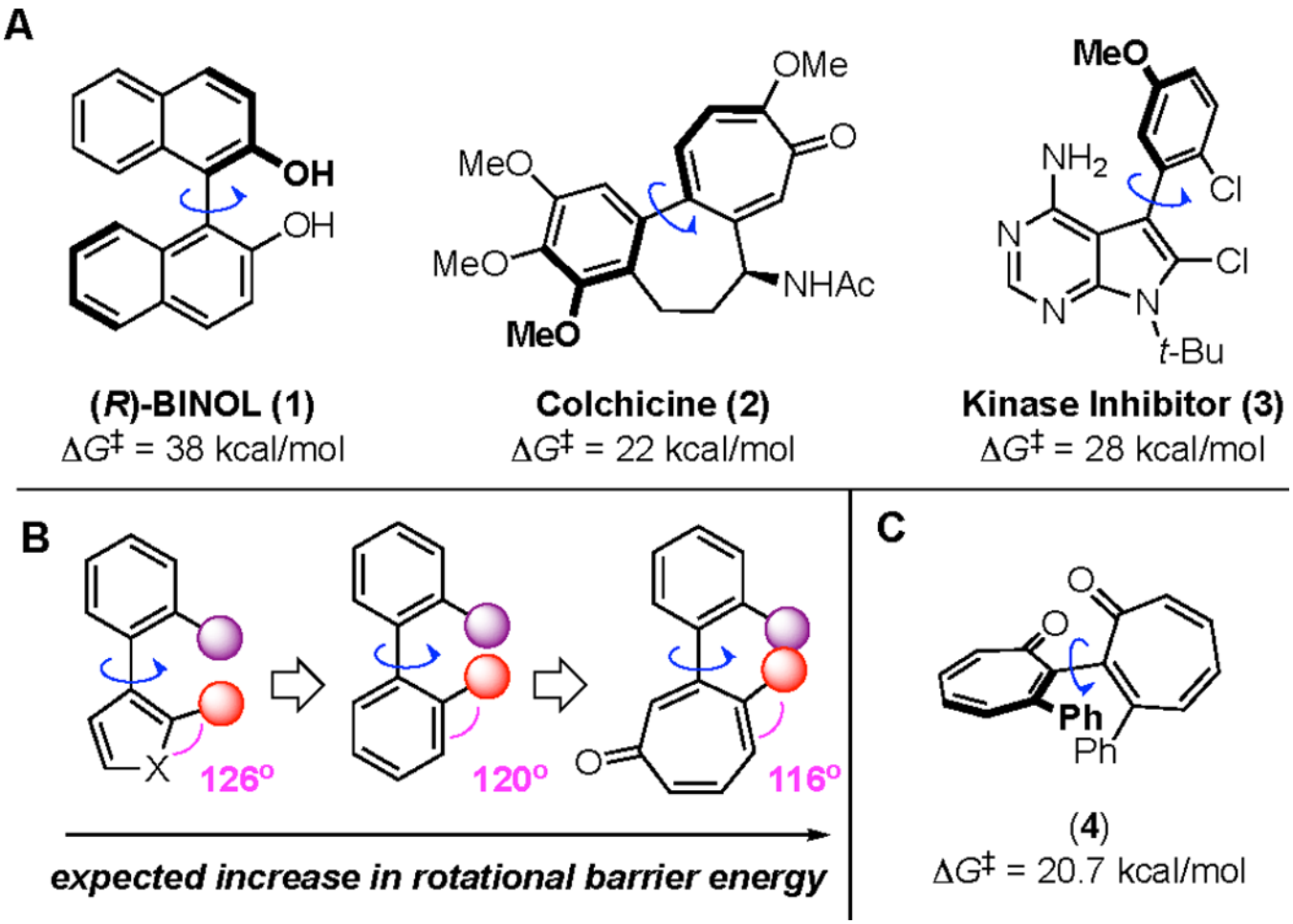

Figure 1. Atropisomerism and troponoids.

(A) Examples of valuable molecules exhibiting atropisomerism. (B) External bond angle differences between 5, 6, and 7-membered aromatic rings, and their influence on proximity of ortho-substituents. (C) Bistropone homodimer **4** with an experimental rotational barrier measurement.

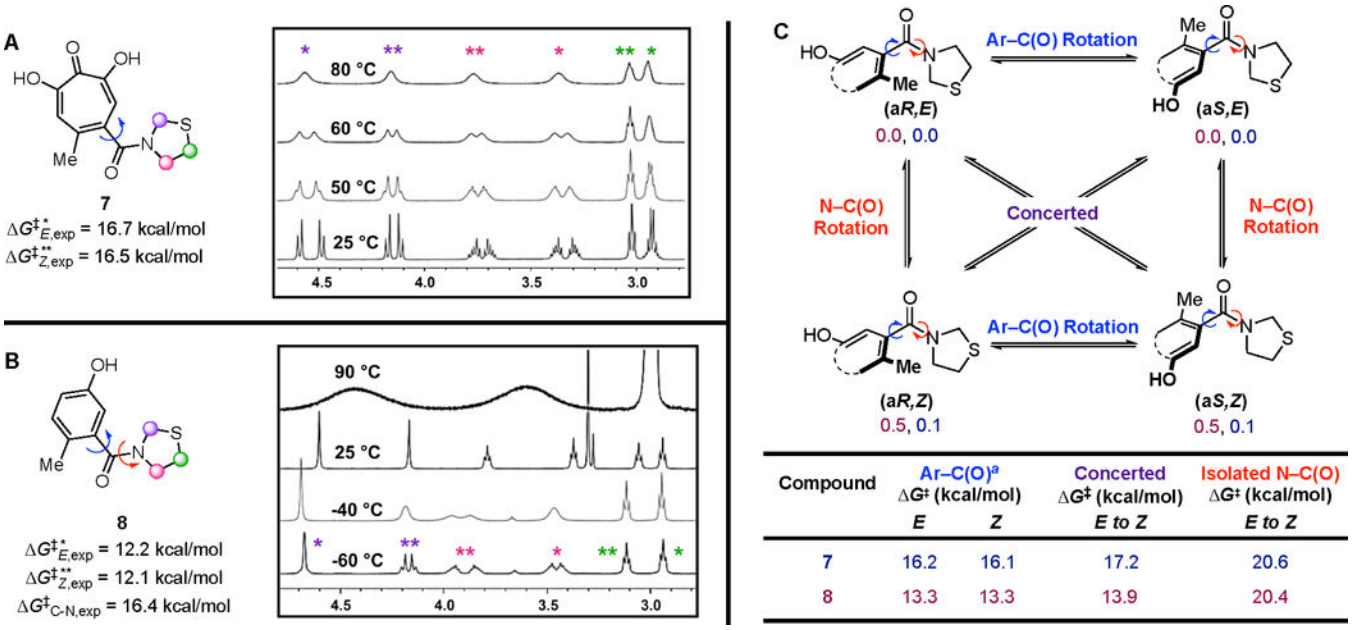

Compound	Ar–C(O)[a] ΔG‡ (kcal/mol)		Concerted ΔG‡ (kcal/mol)	Isolated N–C(O) ΔG‡ (kcal/mol)
	E	*Z*	*E to Z*	*E to Z*
7	16.2	16.1	17.2	20.6
8	13.3	13.3	13.9	20.4

Figure 2.

Variable temperature 1H-NMR spectra of **(A)** troponoid, **7** (DMSO-*d*6), and **(B)** benzamide, **8** (CD_2Cl_2 and DMSO-*d*6) on an Agilent 500 MHz NMR spectrometer. The peaks assigned to the protons of the *Z* and *E* amide conformers are denoted by (*) and (**), respectively. Peak intensities normalized for clarity. **(C)** Proposed pathways to enantiomerization (Ar–C(O) rotation) and amide isomerization (N–C(O) rotation) for differentially substituted thiazolidine systems with energy values (kcal/mol) indicated for ground states, as well as computed rotational barriers denoted in the subsequent table (calculated at the M06–2X-D3/6–311++G(2d,3p) level of theory with using the Gaussian 09 suite). *a* Obtained from considering both isolated Ar-C(O) and concerted pathways.

A

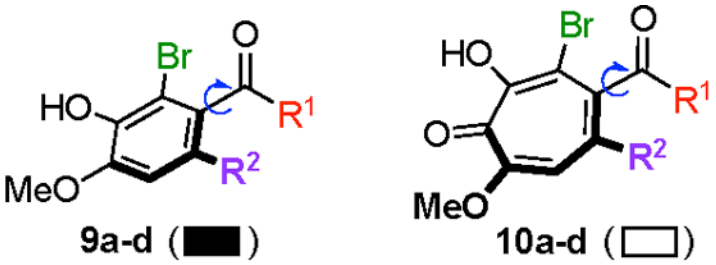

Entry	R1	R2	Benzenoids No.	Benzenoids $t_{1/2}$ (s)	Benzenoids $\Delta G^{\ddagger}$ (kcal/mol)	Troponoids No.	Troponoids $t_{1/2}$ (s)	Troponoids $\Delta G^{\ddagger}$ (kcal/mol)
1	Ph	Me	**9a**	6×10^{-4}	13.4	**10a**	2×10^{2}	20.9
2	$N(CH_2)_5$	H	**9b**	0.2	16.9	**10b**	1×10^{2}	20.5
3	$N(CH_2)_5$	Me	**9c**	5×10^{4}	24.2	**10c**	8×10^{9}	31.2
4	$N(i\text{-}Pr)_2$	Me	**9d**	2×10^{5}	24.9	**10d**	2×10^{11}	33.2

B

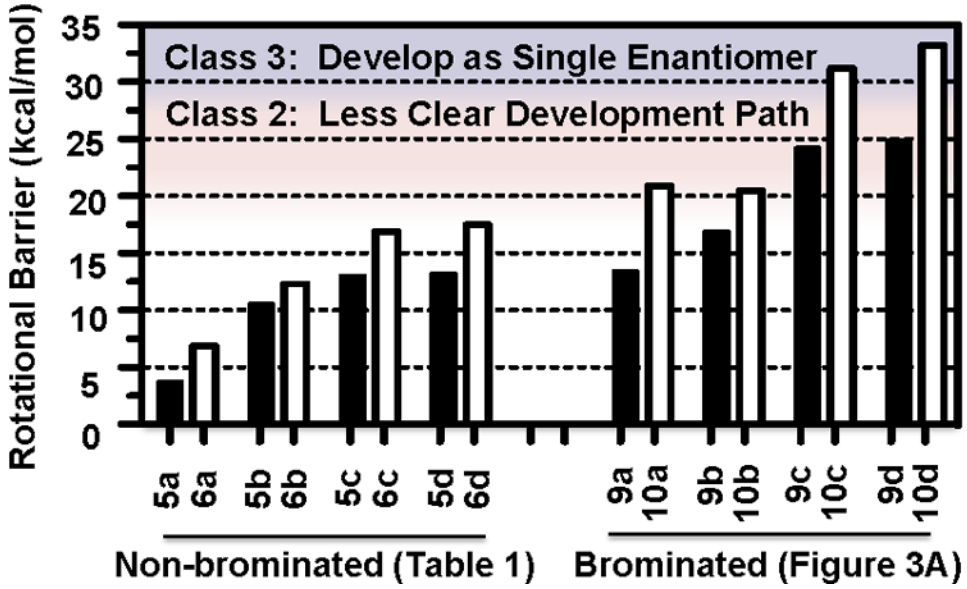

Figure 3.

(A) Computed rotational energy barriers of brominated troponoids and benzenoids, with (B) comparison to non-brominated molecules. Class 2 = intermediate barrier and Class 3 = stable atropisomerism. Rotational barriers were computed at the M06–2X/6–311++G(2d, 3p)//B3LYP/6–31+G(d,p) level of theory at 298.15 K and 1 atm using the Gaussian 09 suite.

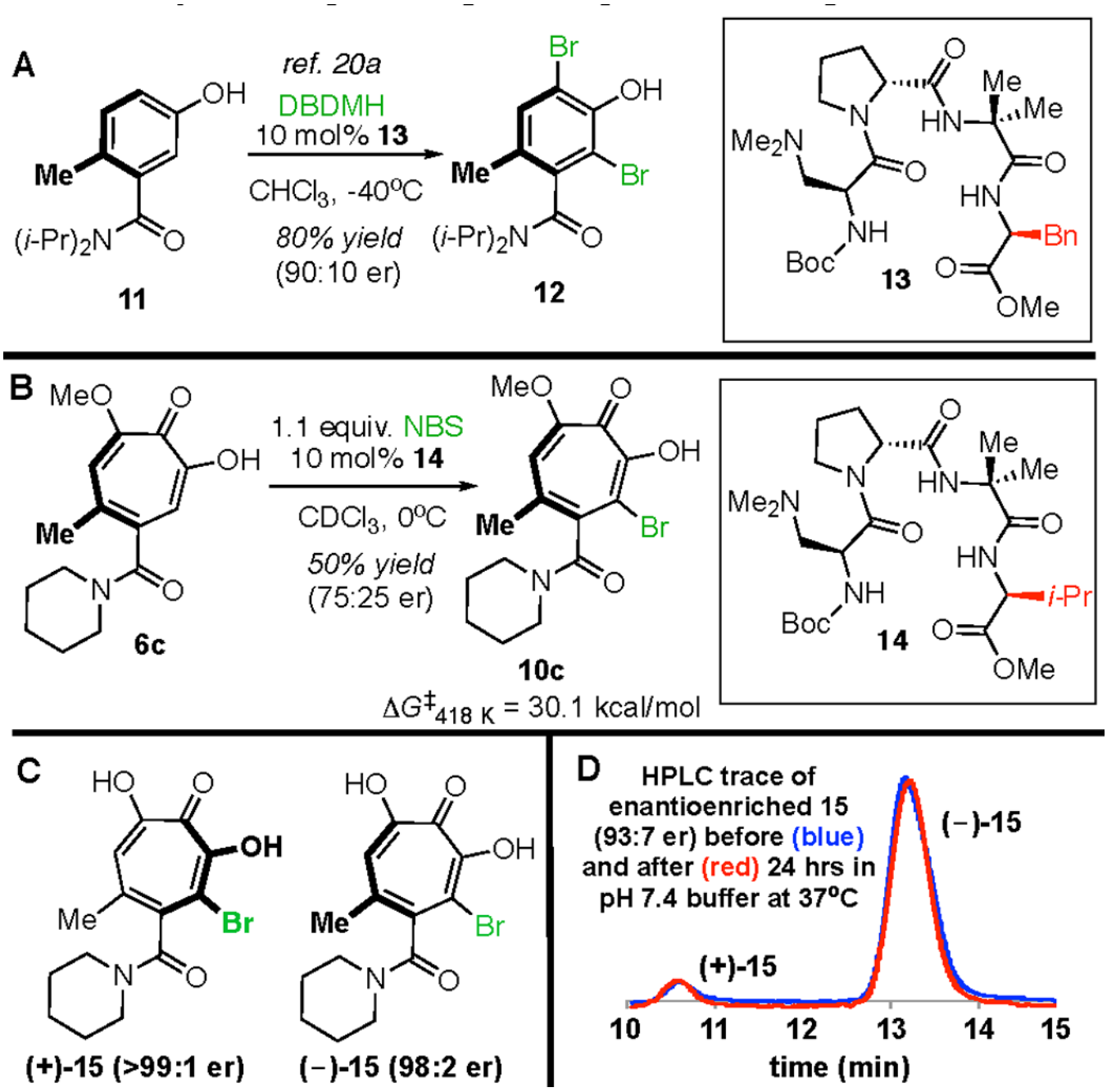

Figure 4.

(A) Atroposelective halogenation of close troponoid structural homolog **11** using peptide **13**. (B) Peptide **14** was found to deliver enantioenriched **10c**. (C) a-Hydroxytropolone atropisomers of **15**. (D) Enantiomerically enriched **(–)-15** before (blue) and after (red) incubation at 37 °C in phosphate buffer (pH = 7.4) as monitored by analytical HPLC (CHIRALPAK® IC, 250 mm, i.d. 4.6 mm, 30% acetonitrile in water with 0.1% TFA, 1.5 mL/min). Peak intensities normalized for clarity.

Table 1.

Computed rotational energy barriers of related troponoids and benzenoids.

Rotational barriers were computed at the M06–2X/6–311++G(2d,3p)//B3LYP/6–31+G(d,p) level of theory at 298.15 K and 1 atm using the Gaussian 09 suite.

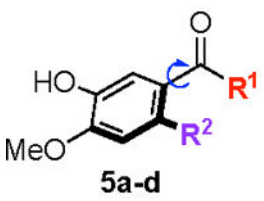

5a-d

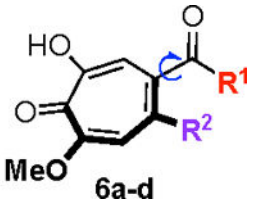

6a-d

			Benzenoids			*Troponoids*		
Entry	**R^1**	**R^2**	**No.**	***t*½ (s)**	**Δ*G*‡ (kcal/mol)**	**No.**	***t*½ (s)**	**Δ*G*‡ (kcal/mol)**
1	Ph	Me	**5a**	6×10^{-11}	3.7	**6a**	1×10^{-8}	6.9
2	$N(CH_2)_5$	H	**5b**	6×10^{-6}	10.5	**6b**	1×10^{-4}	12.3
3	$N(CH_2)_5$	Me	**5c**	4×10^{-4}	13.0	**6c**	0.3	16.9
4	N(*i*-Pr)$_2$	Me	**5d**	5×10^{-4}	13.2	**6d**	0.7	17.5